

JAST (Journal of Animal Science and Technology) TITLE PAGE

Upload this completed form to website with submission

1
2
3

ARTICLE INFORMATION	Fill in information in each box below
Article Type	Research article
Article Title (within 20 words without abbreviations)	Alterations in steroid hormone receptors, angiogenic, cell proliferation, apoptotic, and Ras-related factors during estrous cycle in porcine corpus luteum
Running Title (within 10 words)	Ras related factors in porcine corpus luteum
Author	Hyewon Kim ¹ , Sang-Hee Lee ^{1,2}
Affiliation	¹ College of Animal Life Sciences, Kangwon National University, Chuncheon 24341, Republic of Korea ² School of ICT, University of Tasmania, Hobart, TAS7005, Australia
ORCID (for more information, please visit https://orcid.org)	Sang-Hee Lee (https://orcid.org/0000-0001-8725-4174) Hyewon Kim (https://orcid.org/0009-0007-2496-8912)
Competing interests	No potential conflict of interest relevant to this article was reported.
Funding sources State funding sources (grants, funding sources, equipment, and supplies). Include name and number of grant if available.	This work was supported by Innovative Human Resource Development for Local Intellectualization program through the Institute of Information & Communications Technology Planning & Evaluation (IITP) grant (IIPT-2026-RS-2023-00260267) and 2023 Research Grant from Kangwon National University.
Acknowledgements	Not applicable.
Availability of data and material	Upon reasonable request, the datasets of this study can be available from the corresponding author.
Authors' contributions Please specify the authors' role using this form.	Conceptualization: Lee SH. Data curation: Kim H, Lee SH. Formal analysis: Kim H. Methodology: Kim H. Software: Kim H. Validation: Kim H. Investigation: Kim H, Lee SH. Writing - original draft: Kim H, Lee SH. Writing - review & editing: Kim H, Lee SH.
Ethics approval and consent to participate	The Institutional Animal Care and Use Committee of the Kangwon National University approved all animal procedures (KW-250716-2).

4
5

CORRESPONDING AUTHOR CONTACT INFORMATION

For the corresponding author (responsible for correspondence, proofreading, and reprints)	Fill in information in each box below
First name, middle initial, last name	Sang-Hee, Lee
Email address – this is where your proofs will be sent	sang1799@kangwon.ac.kr
Secondary Email address	
Address	College of Animal Life Sciences, Kangwon National University, Chuncheon 24341, Korea
Cell phone number	+82-10-5366-4179

Office phone number	+82-33-250-8626
Fax number	

6
7

ACCEPTED

8 **Abstract**

9 This study aimed to examine the association of Ras signaling with steroid hormone receptors, angiogenic factors,
10 cell cycle/cell proliferation markers, and apoptotic factors during the estrous cycle in pigs. Porcine corpus luteum
11 (CL) tissues were classified into the early (EP), middle (MP), and late phases (LP). Furthermore, the mRNA and
12 protein expression profiles of steroid hormone receptors, angiogenic factors, cell cycle-related factors, apoptosis-
13 related factors, Ras and Ras GTPases were assessed using reverse transcription-polymerase chain reaction,
14 western blot, and protein–protein interaction. The CL showed the highest tissue weight in the MP. At the mRNA
15 level, *3 β -HSD* and *P4R* were substantially increased at MP, and *PGF2 α R* was markedly elevated at LP. At the
16 protein level, 3 β -HSD was the highest at MP, P4R was increased at EP, and PGF2 α R was the highest at LP. For
17 angiogenic factors, *angiopoietin 1* and *Tie2* mRNA levels were increased in MP, vascular endothelial growth
18 factor D protein levels were increased in MP. Cell cycle factors revealed increased *extracellular signal-regulated*
19 *kinase 1*, *cyclin dependent kinase 1*, and *cyclin B1* mRNA expression in MP, whereas CCNB1 protein expression
20 increased in EP. *tumor necrosis factor receptor 1* mRNA was the highest in LP, *Bax* and *caspase 3* mRNA
21 increased in the MP group, and *Bcl2* mRNA increased at EP. At the protein level, Casp3 was markedly increased
22 in LP. Additionally, the Ras family and Ras GTPases showed stage-dependent expression alterations at the mRNA
23 and protein levels. Search Tool for the Retrieval of Interacting Genes-based molecular action analysis suggested
24 a conserved interaction architecture across species and indicated potential functional linkages connecting hormone
25 receptors and angiogenesis modules with Ras-related components and downstream cell cycle factors. Thus,
26 porcine CL reveals coordinated, phase-dependent alterations in steroidogenic activity, angiogenesis, cell cycle
27 regulation, apoptosis, and Ras-related signaling components during the estrous cycle. In conclusion, these findings
28 provide foundational evidence that Ras signaling pathways act as integrative regulatory modules linking endocrine
29 and vascular cues to intracellular signaling during the estrous cycle. This supports further porcine-specific
30 mechanistic studies to clarify the Ras-centered regulation of CL function.

31

32 **Keywords:** Angiogenesis, Apoptosis, Corpus luteum, Pigs, Ras GTPase

33

34 **Introduction**

35 The corpus luteum (CL), a transient endocrine gland formed following ovulation, plays a crucial role in
36 regulating female reproductive functions by secreting progesterone (P4) [1]. The action of prostaglandin F2 alpha
37 (PGF2 α) secreted from the endometrium under estrogen stimulation causes the blood vessels distributed in the
38 CL to constrict, if pregnancy does not occur. The activity of the cholesterol synthesis enzymes is suppressed,
39 resulting in their degeneration [2]. In mammals, the CL is one of the few adult tissues that undergo rapid formation,
40 functional maturation, and structural regression during each estrous cycle [3]. Dynamic remodeling involves
41 extensive alterations in angiogenesis, cell proliferation, and apoptosis [4].

42 During the initial CL formation stage, ovulation triggers extensive vascular invasion, whereby blood vessels
43 originating from the theca layer rapidly penetrate the ruptured follicles' granulosa compartment [5]. This newly
44 established vascular network facilitates the efficient delivery of cholesterol and endocrine signals necessary for
45 steroidogenesis [6]. Luteal cells differentiated from granulosa and theca cells synthesize P4 using cholesterol
46 stored in the cytoplasmic lipid droplets, thereby supporting luteal endocrine function [7]. PGF2 α secreted from
47 the uterus disrupts luteal blood flow and steroidogenic activity in the absence of pregnancy, thereby initiating
48 functional and structural luteal regression [8]. Consequently, the luteal tissue undergoes atrophy accompanied by
49 lipid degeneration of luteal cells, ultimately forming the corpus albicans [9]. The integrative mechanisms
50 coordinating angiogenesis, steroidogenesis, cell proliferation, and apoptosis during the estrous cycle in pigs
51 remain elusive, although these regulatory components have been individually described.

52 Cell cycle progression and proliferation are fundamental processes that support rapid growth and functional
53 establishment of the CL during the estrous cycle [10]. After ovulation, luteal cells actively proliferate to expand
54 luteal tissue mass and acquire full steroidogenic capacity, a process tightly regulated by key cell-cycle-associated
55 factors, including cyclin B1 (CCNB1), cyclin-dependent kinase 1 (CDK1), and the mitogen-activated protein
56 kinases/extracellular signal-regulated kinase (MAPK/ERK) signaling components ERK1 and MAPK1 [11]. The
57 activation of the MAPK/ERK pathway facilitates proliferation and differentiation of the luteal cell, thereby
58 promoting luteal maturation and P4 production [11]. Contrastingly, dysregulation of this pathway disrupts
59 folliculogenesis and luteinization [12]. As the estrous cycle advances, proliferative activity progressively declines
60 and apoptotic signaling becomes dominant, driving structural and functional regression of the luteal cell [13]. The
61 balance between pro-apoptotic factors (tumor necrosis factor receptor 1; TNFR1, Bax, and caspase 3; Casp3) and
62 anti-apoptotic proteins, such as Bcl2, ultimately determines luteal cell survival and CL lifespan [14].

63 Ras and Ras guanosine triphosphatases (GTPases) are small GTP-binding proteins that act as molecular
64 switches to control intracellular signaling associated with proliferation, differentiation, and survival [15]. Ras
65 guanine nucleotide exchange factors (Ras GEFs), such as the son of sevenless homolog 1 (SOS1), mediate Ras
66 activation whereas Ras GTPase-activating proteins (Ras GAPs), including neurofibromatosis type 1 (NF1) and
67 Ras p21 protein activator 1 (RASA1), govern inactivation [16]. These regulatory proteins converge on major
68 signaling cascades, such as the MAPK/ERK and PI3K/AKT-pathways known to affect ovarian follicular growth,
69 steroid hormone production, angiogenesis, and cell-cycle regulation [17]. Although Ras-mediated signaling has
70 been assessed in several reproductive tissues, studies particularly addressing Ras's role and its GTPases in porcine
71 CL physiology remain limited. Considering the rapid structural alterations and high metabolic demands of the CL,
72 Ras signaling may be a key integrative regulator linking angiogenesis, steroidogenesis, and cellular turnover [18].

73 However, Ras and its GTPases during the estrous cycle in porcine CL have not been clearly defined. No
74 comprehensive investigation has been conducted to compare the expression of Ras family members (H-, K-, N-,
75 and R-Ras) and their regulatory proteins across distinct estrous cycles. Additionally, the potential interactions
76 among Ras GTPases, steroid hormone receptors, and angiogenic factors have not been examined in pigs.
77 Understanding these molecular relationships is critical because Ras signaling pathways may affect the transition
78 from proliferation and steroidogenesis in the early phase (EP) and middle phase (MP) to apoptosis and regression
79 in the late phase (LP) [19].

80 Pigs and humans share key reproductive characteristics, including ovarian follicular dynamics, steroid
81 hormone profiles, angiogenic mechanisms, and the balance between proliferative and apoptotic signals during the
82 development and regression of CL [20, 21]. These similarities improve the translational value of porcine studies
83 for understanding human ovarian physiology, estrous cycle deficiency, and early pregnancy loss. From a practical
84 perspective, elucidating the CL function in pigs contributes to improved reproductive management in the swine
85 industry, supporting enhancements in estrous synchronization, fertility monitoring, and pregnancy diagnosis [22].
86 Additionally, the characterization of steroidogenesis, angiogenesis, and cell turnover in the porcine CL provides
87 fundamental insights into the biology of a rapidly remodeling endocrine gland [23, 24]. Thus, porcine CL research
88 has agricultural and biomedical significance, strengthening its role as a model for mammalian reproductive
89 physiology.

90 The angiogenic [25], steroidogenic [26], cell proliferation [27], and apoptotic [28] pathways are dynamically
91 regulated during CL development and regression in pigs. Ras and its GTPases function as the primary molecular
92 switches that control intracellular signaling associated with cell proliferation [29], differentiation [30],

93 angiogenesis [31], and apoptosis [32, 33] in different reproductive tissues. Considering these observations,
94 together with the rapid structural remodeling and high metabolic demands of the CL, we hypothesized that Ras-
95 related signaling pathways play an integrated role in coordinating luteal development and regression in pigs. We
96 investigated the phase-dependent expression patterns of the Ras family members (H-, K-, N-, and R-Ras) and their
97 regulatory proteins (NF1, RASA1, and SOS1) in the porcine CL during the EP, MP, and LP. Furthermore, we
98 simultaneously examined the mRNA and protein expression levels of hormone receptors, angiogenic markers,
99 cell cycle regulators, and apoptotic factors. Pathway-level protein–protein interaction (PPI) analysis was
100 performed using the Search Tool for the Retrieval of Interacting Genes (STRING) database to further elucidate
101 the molecular relationships underlying these regulatory processes. Additionally, we aimed to clarify the potential
102 involvement of Ras-related signaling in integrating angiogenesis, steroidogenesis, cell proliferation, and apoptosis
103 during the porcine estrous cycle.

104

105 **Materials and Methods**

106 **Animals and CL collection**

107 The Institutional Animal Care and Use Committee of the Kangwon National University approved all animal
108 procedures (KW-250716-2). Porcine CL were collected at a local slaughterhouse (Pochen farm, Pocheon,
109 Republic of Korea) and transported to the laboratory at 4°C within 2 h following slaughter. The estrous cycle
110 phase was assigned primarily based on ovarian and CL morphology in the laboratory (Fig. 1A–C). The CL of EP
111 were defined as samples showing visible red blood within the CL, having a relatively smaller overall size than
112 MP CL, and showing blood inside the tissue after isolation and dissection (Fig. 1A). The CL of MP were defined
113 as samples in which blood was not observed and which showed a pinkish luteal coloration (Fig. 1B). The CL of
114 LP were defined as samples with a smaller tissue size than MP CL and ovaries containing developing follicles
115 (Fig. 1C). The expression patterns of *3 β -hydroxysteroid dehydrogenase (3 β -HSD)* and *prostaglandin F2 alpha*
116 *receptor (PGF2aR)* were examined only as supportive biological indicators of luteal functional status and were
117 not used for marker-based reclassification of the samples (Fig. 1E and 1F). Subsequently, all isolated CL tissues
118 were weighed and stored at –80°C until further use.

119

120 **RNA extraction and cDNA synthesis**

121 Total RNA was extracted using RNAiso Plus (Takara, Tokyo, Japan), according to the manufacturer's
122 protocol. RNA quality and concentration were measured using an EzDrop 1000C spectrophotometer (Blue-Ray
123 Biotech, New Taipei City, Taiwan). Next, 5.0 µg RNA was utilized to synthesize cDNA using a SuPrimeScript
124 cDNA Synthesis Kit (Genetbio, Daejeon, Republic of Korea) according to the manufacturer's instructions.
125 Furthermore, cDNA was stored at -18°C until reverse transcriptase polymerase chain reaction (RT-PCR).

126

127 **Real-Time PCR**

128 Using a qPCR system (Quant3 Studio, Applied Biosystems, Thermo Fisher Scientific, USA), cDNA, along
129 with qPCR mix, primers, and ddH₂O, was amplified. Amplification conditions included incubation at 50 °C for
130 2 min, initial denaturation at 95 °C for 10 min, followed by 40 cycles of denaturation at 95 °C for 15 s and
131 annealing/extension at 60 °C for 1 min. The mRNA expression levels were normalized to that of *β-actin* mRNA.
132 All reactions were performed in triplicate. Primer specificity was confirmed by melt curve analysis. Table 1 lists
133 the primer sequences used in the experiments. We computed the relative mRNA expression levels using the
134 comparative cycle threshold ($2^{-\Delta\Delta C_t}$) method [34].

135

136 **Western blot**

137 Luteal tissues were lysed in radio-immunoprecipitation assay cell lysis buffer (GenDEPOT, Barker, TX,
138 USA) containing inhibitors (Xpert protease inhibitor cocktail solution and Xpert phosphatase inhibitor cocktail
139 solution; GenDEPOT). The resulting homogenate was centrifuged at 12,000 rpm ($13,523 \times g$) and 4 °C for 20
140 min and the supernatants were collected in a fresh tube. Total protein concentration was measured using the Pierce
141 Bicinchonic Acid Protein Assay Kit-Reducing Agent Compatible, according to the manufacturer's protocol
142 (23250; Thermo Fisher Scientific). Proteins were separated using sodium dodecyl sulfate-polyacrylamide gel
143 electrophoresis and transferred onto polyvinylidene difluoride membranes (Millipore, Burlington, MA, USA)
144 using a Trans-Blot turbo rapid transfer system (1704150, Bio-Rad, Hercules, CA, USA), according to the
145 manufacturer's protocol. The membranes were blocked in blocking solution (5% skim milk in Tris-buffered
146 saline/0.5% Tween-20; TBS-T) at room temperature for 1 h. After blocking membranes, the membranes incubated
147 overnight at 4 °C with the appropriate primary antibodies (Table 2). Images were acquired using a
148 chemiluminescence substrate (W3651-012; GenDEPOT) and quantified using a chemiluminescence imaging

149 system (UVITEC Alliance MINI HD9 system, UVITEC, Britain). Band intensities were quantified by
150 densitometric analysis and normalized to β -actin as a loading control.

151

152 **Bioinformatics analysis**

153 Protein–protein interaction and functional association networks were constructed using the STRING [35]
154 (v.10.0; <http://string.embl.de>) database, with *Sus scrofa* selected as the target species. Network edges were
155 generated using a medium confidence score cutoff of 0.400. The molecular action view was used to visualize
156 predicted interaction modes, including positive and negative interactions, activation, and inhibition. STRING-
157 derived interactions were interpreted as predicted functional associations rather than experimentally validated
158 causal relationships. Subsequently, the molecular action of the Ras GTPases (NF1, RASA1, and SOS1), hormone
159 receptors (progesterone receptor; P4R, prostaglandin F2 alpha receptor; PGF2 α R, and estrogen receptor alpha;
160 ER α), angiogenesis factors (vascular endothelial growth factor A; VEGFA, VEGF receptor 2; VEGFR2,
161 angiopoietin 1; Ang1, and Tie2), apoptosis factors (TNFR1, Bax, and Casp3), and Ras proteins (H-Ras, K-Ras,
162 N-Ras, and R-Ras) were examined using the STRING database.

163

164 **Statistical analysis**

165 Each experiment was conducted with at least three replications. Data was analyzed using SAS ver. 9.4 (SAS
166 Institute, Cary, NC, USA). Data was presented as the mean \pm standard error of the mean (SEM) and differences
167 between each group (EP vs MP, MP vs LP, and EP vs LP) were calculated using Student's t-test. Statistical
168 significance was set at $p < 0.05$.

169

170 **Results**

171 **Morphological characteristics, tissue weight, and expression of the steroid hormone receptors in the porcine** 172 **ovary during the estrous cycle**

173 Fig. 1 shows the morphological characteristics of the porcine ovaries at the EP (Fig. 1A), MP (Fig. 1B),
174 and LP (Fig. 1C) stages of the estrous cycle. The CL showed a substantial increase in size during the MP compared
175 with that during the EP and LP. Consistent with these morphological observations, the tissue weight of the CL
176 (Fig. 1D) was significantly higher in the MP than in the EP and LP ($p < 0.001$).

177 Fig. 1E and 1F show the relative expression levels of the steroid hormone receptors. At the mRNA level
178 (Fig. 1E), the *3β-HSD* and *P4R* expressions were significantly increased at the MP compared with the EP and LP,
179 whereas *ERα* mRNA expression did not significantly differ during the estrous cycle. Contrastingly, *PGF2αR*
180 mRNA expression was significantly higher at the LP than at the EP and MP ($p < 0.05$). At the protein level (Fig.
181 1F), 3β-HSD protein expression was the highest at the MP, whereas P4R protein expression was elevated at the
182 EP ($p < 0.001$). Similar to the mRNA results, ERα protein expression did not reveal significant differences among
183 the stages, whereas PGF2αR protein expression was significantly increased at the LP ($p < 0.05$).

184

185 **Expression of angiogenesis, cell cycle, and apoptosis-related factors**

186 Fig. 2A-D show the expression of the angiogenesis-and cell cycle-related factors in the porcine CL during
187 the estrous cycle. The *VEGFA* and *VEGF receptor 2 (VEGFR2)* mRNA expression levels (Fig. 2A) were not
188 markedly different among the EP, MP, and LP groups. Contrastingly, the mRNA expression levels of *angiopoietin*
189 *1 (Ang1)* and *Tie2* were significantly higher in the MP than in the EP and LP ($p < 0.05$). At the protein level (Fig.
190 2B), vascular endothelial growth factor D (VEGFD) protein expression was significantly higher at the MP than at
191 the EP and LP ($p < 0.05$), whereas angiopoietin 4 (Ang4) protein expression did not significantly differ during the
192 estrous cycle. Tie2 protein expression did not significantly differ during the estrous cycle. The mRNA expression
193 levels of *ERK1*, *CDK1*, and *CCNB1* (Fig. 2C) were significantly higher in the MP group than in the EP and LP
194 groups ($p < 0.05$), whereas *MAPK1* mRNA expression did not significantly differ during the estrous cycle. At the
195 protein level (Fig. 2D), the expression levels of ERK1/2 and phosphorylated ERK1/2 (p-ERK1/2) were not
196 significantly different among EP, MP, and LP, whereas CCNB1 protein expression was significantly higher in the
197 EP than in the MP and LP ($p < 0.05$). Fig. 2E and 2F illustrate the expression patterns of the apoptosis-related
198 factors. *TNFR1* mRNA expression levels (Fig. 2E) were significantly higher in the LP group than in the EP and
199 MP groups ($p < 0.05$). Contrastingly, the mRNA expression levels of *Bax* and *Casp3* were significantly increased
200 in MP, whereas *Bcl2* mRNA expression was significantly higher in EP than in MP and LP ($p < 0.05$). At the
201 protein level (Fig. 2F), the expression levels of TNFR1, Bax, and Bcl2 were not significantly different during the
202 estrous cycle, whereas Casp3 protein expression was significantly higher in the LP than in the EP and MP ($p <$
203 0.05).

204

205 **Re-validation of the Ras family members and alterations in the Ras-related regulatory factors by mRNA**
206 **and protein expression in the porcine corpus luteum**

207 The expression of Ras family members and GTPases identified in the porcine CL was re-validated using
208 mRNA and protein analyses (Fig. 3). The mRNA levels of *H-Ras*, *K-Ras*, *N-Ras*, and *R-Ras* were significantly
209 changed during the estrous cycle (Fig. 3A). Compared to EP, the expression of Ras family mRNAs revealed
210 significant alterations in MP and was significantly decreased in LP ($p < 0.05$). Similarly, the protein expression
211 levels of H-Ras, K-Ras, and R-Ras were significantly altered during the estrous cycle, with higher expression
212 noted in the MP and decreased expression in the LP than in the EP ($p < 0.05$; Fig. 3B). The mRNA expression
213 levels of *NF1*, *RASA1*, and *SOS1* were not significantly different between the EP and MP, but were significantly
214 changed in the LP ($p < 0.05$; Fig. 3C). At the protein level, the expression of NF1, RASA1, and SOS1 revealed
215 significant stage-dependent alterations, with changed expression noted in the MP and LP compared to the EP (p
216 < 0.05 ; Fig. 3D).

217

218 **Molecular actions in the hormone receptors, angiogenesis, cell cycle, apoptosis, Ras GTPases, and Ras** 219 **protein**

220 Fig. 4 shows the molecular actions of hormone receptors, angiogenic factors, cell cycle-related factors,
221 apoptotic factors, Ras GTPases, and Ras GTPase proteins. STRING-based molecular action networks were
222 constructed using the same set of proteins arranged in the same positions in *Homo sapiens* (Fig. 4A), *Mus*
223 *musculus* (Fig. 4B), *Bos taurus* (Fig. 4C), and *Sus scrofa* (Fig. 4D) to compare conserved interaction patterns
224 across major mammalian models. In the network, ER α was predicted to have a potential activating relationship
225 with P4R (Fig. 4, green arrows), and ER α was also connected to the angiogenic module via VEGFA and its
226 receptor VEGFR2. Additionally, the angiogenic receptors VEGFR2 and Tie2 were associated with Ras-related
227 signaling through SOS1 (Fig. 4, green arrows), suggesting that these molecules may represent candidate links
228 between angiogenic signaling and Ras-related pathways in porcine CL.

229 Moreover, the STRING molecular action map indicated that H-Ras and R-Ras were functionally connected to
230 angiogenic receptors and SOS1, suggesting a potential network-level association between angiogenic signaling
231 and Ras GTPase-related pathways (Fig. 4, green arrows). However, Ras GAP (NF1 and RASA1) were predicted
232 to have inhibitory relationships with Ras signaling components (Fig. 4, red lines). Furthermore, Ras-related nodes
233 were located at the interface between upstream hormone receptor/angiogenesis modules and downstream cell
234 cycle (cell proliferation) factors (MAPK1, ERK1, CDK1, and CCNB1) via multiple interaction links (Fig. 4, gray
235 lines). Contrastingly, apoptotic factors (TNFR1, Bax, Bcl2, and Casp3) were primarily connected within the
236 apoptosis module and revealed relatively limited positive molecular interactions with hormone receptors,

237 angiogenic factors, and Ras-related factors in the network (Fig. 4). Thus, although the overall architecture of these
238 interaction modules is broadly conserved across four species, experimental evidence validating how these
239 conserved connections operate in porcine CL is limited. Therefore, combining the species comparative network
240 with stage-dependent expression profiles supports the requirement of porcine-specific studies to clarify the Ras-
241 centered regulatory mechanisms coordinating angiogenesis, cell cycle transition, and luteal regression.

242

243 Discussion

244 The CL is a transient endocrine tissue that undergoes rapid formation, functional maintenance, and
245 regression during the estrous cycle, which requires the coordinated regulation of steroidogenesis, vascular
246 remodeling, cell cycle transition, and apoptotic signaling [36, 37]. Thus, we assessed stage-dependent variations
247 in gross morphology and tissue weight, along with the expression profiles of steroid hormone receptor-related
248 factors, angiogenesis- and cell cycle-related factors, apoptosis-related markers, and Ras-related components in the
249 porcine CL, and further integrated these data using a STRING-based molecular action network.

250 Morphological features and tissue weight data indicated that the porcine CL reached its maximal growth
251 during MP [38]. This observation was supported by 3 β -HSD's expression pattern, which revealed the highest
252 expression at the MP at the mRNA and protein levels [39]. This suggests that the MP corresponds to the period
253 of improved steroidogenic capacity [40]. Additionally, *P4R* mRNA increased in the MP, whereas P4R protein
254 increased in the EP. Although mRNA and protein levels do not always exhibit identical patterns, this discrepancy
255 suggests that P4 signaling in porcine CL may be regulated at multiple levels, especially during early luteal
256 development. Contrastingly, ER α did not exhibit considerable differences across estrous cycle at either the mRNA
257 or protein level in the present dataset. This indicates that ER α expression itself may remain relatively stable during
258 the estrous cycle. Notably, PGF2 α R was the highest at the LP at the mRNA and protein levels, which is consistent
259 with an elevated luteolytic responsiveness as the CL transitions toward regression [41]. Nevertheless, although
260 the expression patterns of 3 β -HSD and PGF2 α R were consistent with the expected biological characteristics of
261 MP and LP, respectively, 3 β -HSD expression alone cannot be regarded as a direct measure of P4 production.
262 Therefore, the interpretation of steroidogenic capacity based on 3 β -HSD expression should be considered with
263 caution. In future studies, particularly IHC-based analyses of Ras protein distribution in porcine CL tissues across
264 the estrous cycle, P4 production in each sample will be quantified by ELISA to more accurately confirm the
265 physiological status of the samples prior to further analysis.

266 Angiogenesis is necessary for CL formation and function, because the developing luteal tissue needs rapid
267 vascularization and subsequent stabilization [17]. In the present study, the angiogenic factors exhibited marker-
268 and level-dependent patterns. *VEGFA*, *VEGFR2*, and *Ang1* were analyzed at the mRNA level, whereas *VEGFD*
269 and *Ang4* was evaluated at the protein level, primarily due to practical considerations such as assay availability
270 and antibody specificity. At the mRNA level, *VEGFA* and *VEGFR2* did not reveal considerable variations among
271 the stages, whereas *Ang1* and *Tie2* were elevated in the MP. At the protein level, *VEGFD* was increased in the
272 MP. Additionally, *Ang4* and *Tie2* protein did not reveal significant variations among the stages. Thus, luteal
273 vascular remodeling in pigs may be supported by distinct angiogenic mediators depending on the estrous cycle
274 and molecular level. Additionally, the Ang-Tie axis and VEGF family members may contribute in a
275 complementary but not identical way across development and regression.

276 With respect to cell cycle regulation, the mRNA expression of *ERK1*, *CDK1*, and *CCNB1* increased in the
277 MP, whereas *MAPK1* mRNA did not significantly vary among the stages. However, at the protein level, *ERK1/2*
278 and p-*ERK1/2* were not significantly different, whereas *CCNB1* protein was increased in the EP. Although these
279 patterns appear to be partially inconsistent at the molecular level, such variations can occur because complex
280 regulatory steps, including translation efficiency, phosphorylation dynamics, and protein turnover, control cell
281 cycle progression [42]. Therefore, the present findings indicate that the transcriptional activation of cell cycle
282 regulators is prominent during MP, whereas protein level alterations may reflect earlier proliferative cues or
283 differences in stability/processing during early luteal development.

284 Regarding apoptotic regulation, stage-dependent changes were noted that differed between transcripts and
285 proteins. At the mRNA level, *TNFR1* increased in the LP, *Bax* and *Casp3* increased in the MP, and *Bcl2* increased
286 in the EP. At the protein level, *Casp3* was increased in the LP, whereas *TNFR1*, *Bax*, and *Bcl2* did not reveal
287 substantial differences during the estrous cycle. Thus, the transcriptional priming of apoptosis-related factors can
288 be observed earlier; however, the execution marker (*Casp3*) becomes more evident at the protein level during LP,
289 which is consistent with the structural regression occurring during luteolysis. Although not all apoptotic markers
290 revealed substantial protein level alterations, the combined expression profiles support the concept that luteal
291 regression involves a shift toward progressive signaling as the cell cycle progresses.

292 Ras-related signaling regulates cell proliferation, differentiation, and survival through pathways such as
293 the MAPK/ERK pathway [43]. It reported that Ras and its GTPases genes dynamic are changed during estrous
294 cycle in porcine cumulus cell [44], but estrous cycle regulation in porcine CL has not been clearly shown. Herein,
295 Ras family members (H-, K-, N-, and R-Ras), Ras GEF (*SOS1*), and Ras GAP (*NF1* and *RASA1*) revealed

296 differential expression across the estrous cycle at the mRNA and protein levels. These data provide evidence that
297 Ras-related components are dynamically regulated during the porcine estrous cycle and may be linked to luteal
298 functional transition, especially during periods of rapid growth and functional maintenance. Although expression
299 profiling alone does not confirm the direct activation states, these patterns support the requirement for further
300 mechanistic validation of Ras-centered signaling in the luteal cells. Such mRNA-protein discordances observed
301 across multiple targets in this study may be attributed to several study-specific factors, including post-
302 transcriptional regulation, differences in protein turnover and stability between estrous phases, and tissue-level
303 heterogeneity inherent to bulk CL samples composed of mixed luteal, vascular, and immune cell populations. In
304 addition, sampling difference among individual CL and potential sensitivity limitation of estrous phase
305 classification based on ovarian morphology may have contributed to the observed discrepancies. It should also be
306 noted that the present study measured total receptor expression levels at the mRNA and protein level, which do
307 not directly reflect receptor activation or transcriptional activity. Localization analyses such as
308 immunohistochemistry (IHC) or immunofluorescence would be necessary to confirm cell-type-specific
309 expression pattern and functional receptor engagement and are a priority for future studies.

310 Additionally, the STRING-based molecular action network provided an integrated framework for
311 visualizing predicted functional associations among hormone receptor signaling, angiogenesis-related factors,
312 cell-cycle modules, apoptosis-related nodes, and Ras-related factors. The same protein set was visualized in the
313 same arrangement across *Homo sapiens*, *Mus musculus*, *Bos taurus*, and *Sus scrofa*. The network predicted
314 potential associations among ER α -P4R, angiogenic receptors (VEGFR2 and Tie2), the Ras activator SOS1, and
315 Ras family proteins, whereas inhibitory relationships were predicted through NF1 and RASA1. Additionally, Ras-
316 related nodes appeared to occupy intermediate network positions connecting the upstream hormone/angiogenesis
317 modules with downstream cell cycle factors (ERK/MAPK-related nodes, CDK1, and CCNB1). Contrastingly,
318 apoptosis-related factors showed revealed relatively limited positive molecular actions with the hormone receptor
319 angiogenesis-Ras modules in the network. Thus, experimental validation in porcine luteal tissue is still limited,
320 although the general architecture of these interactions is conserved across the four species. Additionally, porcine-
321 specific studies are necessary to determine whether these Ras-centered regulatory mechanisms coordinate
322 angiogenesis, cell cycle transition, and luteal regression in the CL.

323 Although the porcine CL used in this study were classified according to estrous phase, not all genes and
324 proteins examined showed fully consistent phase-dependent patterns. This may partly reflect the biological
325 heterogeneity of CL in polyovulatory pigs and the independent nature of samples collected from slaughtered

326 animals. In future studies, including IHC-based analyses of Ras protein distribution in porcine CL tissues across
327 the estrous cycle, P4 production in each sample will be measured by ELISA to more accurately confirm the
328 physiological status of the samples before further analysis.

329 In summary, this study demonstrated that porcine luteal development and regression are accompanied by
330 coordinated changes in morphology and tissue weight, stage-dependent expression patterns of steroid hormone
331 receptors, and distinct profiles of angiogenesis, cell cycle, and apoptosis-related markers. Moreover, Ras family
332 members change together with comparative network-based molecular actions. This suggests that Ras signaling
333 may function as an integrative module that links endocrine and vascular cues to intracellular growth and survival
334 pathways during the porcine estrous cycle. These results provide fundamental information for future studies aimed
335 at validating Ras-related mechanisms in luteal cells and enhancing our understanding of luteal physiology in pigs.

336

337 **Conclusions**

338 This study showed clear phase-dependent alterations in the porcine CL during the estrous cycle, as evidenced
339 by the morphology, tissue weight, and coordinated expression profiles of the key regulatory factors. CL
340 demonstrated maximal growth at the MP, accompanied by increased *3β-HSD* expression, supporting improved
341 steroidogenic capacity during functional maintenance. Contrastingly, *PGF2αR* expression was the highest at the
342 LP, indicating elevated luteolytic responsiveness during regression. Overall, these results provide fundamental
343 evidence that Ras-related signaling components are dynamically regulated in the porcine CL. Additionally, the
344 findings support the requirement for porcine-specific mechanistic studies to clarify how endocrine and vascular
345 cues coordinate luteal development and regression.

346

347 **Acknowledgments**

348 This work was supported by Innovative Human Resource Development for Local Intellectualization program
349 through the Institute of Information & Communications Technology Planning & Evaluation (IITP) grant (IIPT-
350 2026-RS-2023-00260267), the National Research Foundation of Korea (NRF) grant (RS-2024-00356057) funded
351 by the Korea government (MSIT), and 2023 Research Grant from Kangwon National University.

352

353

354 **References**

- 355 1. Soede NM, Langendijk P, Kemp B. Reproductive cycles in pigs. *Anim Reprod Sci.* 2011;124(3-4):251-8.
356 <https://doi.org/10.1016/j.anireprosci.2011.02.025>
- 357 2. Ziecik AJ, Przygodzka E, Jalali BM, Kaczmarek MM. Regulation of the porcine corpus luteum during
358 pregnancy. *Reproduction.* 2018;156(3):R57-R67. <https://doi.org/10.1530/REP-17-0662>
- 359 3. Devoto L, Fuentes A, Kohen P, Céspedes P, Palomino A, Pommer R, et al. The human corpus luteum: life
360 cycle and function in natural cycles. *Fertil Steril.* 2009;92(3):1067-79.
361 <https://doi.org/10.1016/j.fertnstert.2008.07.1745>
- 362 4. Stocco C, Telleria C, Gibori G. The molecular control of corpus luteum formation, function, and regression.
363 *Endocr Rev.* 2007;28(1):117-49. <https://doi.org/10.1210/er.2006-0022>
- 364 5. Selye H, Friedman SM. The action of various steroid hormones on the Ovary. *Endocrinology.*
365 1940;27(6):857-66. <https://doi.org/10.1210/endo-27-6-857>
- 366 6. Hünigen H, Bisplinghoff P, Plendl J, Bahramsoltani M. Vascular dynamics in relation to immunolocalisation
367 of VEGF-A, VEGFR-2 and Ang-2 in the bovine corpus luteum. *Acta Histochem.* 2008;110(6):462-72.
368 <https://doi.org/10.1016/j.acthis.2008.02.006>
- 369 7. Brüßow K-P, Schneider F, Nürnberg G. Alteration of gonadotrophin and steroid hormone release, and of
370 ovarian function by a GnRH antagonist in gilts. *Anim Reprod Sci.* 2001;66(1-2):117-28.
371 [https://doi.org/10.1016/S0378-4320\(01\)00093-8](https://doi.org/10.1016/S0378-4320(01)00093-8)
- 372 8. Christenson L, Anderson L, Ford S, Farley D. Luteal maintenance during early pregnancy in the pig: role for
373 prostaglandin E2. *Prostaglandins.* 1994;47(1):61-75. [https://doi.org/10.1016/0090-6980\(94\)90075-2](https://doi.org/10.1016/0090-6980(94)90075-2)
- 374 9. Jin X, Xiao L-J, Zhang X-S, Liu Y-X. Apoptosis in ovary. *Front Biosci.* 2011;3:680-97.
375 <https://doi.org/10.2741/s180>
- 376 10. Bertoli C, Skotheim JM, De Bruin RA. Control of cell cycle transcription during G1 and S phases. *Nat Rev*
377 *Mol Cell Biol.* 2013;14(8):518-28. <https://doi.org/10.1038/nrm3629>
- 378 11. Sun Y, Liu W-Z, Liu T, Feng X, Yang N, Zhou H-F. Signaling pathway of MAPK/ERK in cell proliferation,
379 differentiation, migration, senescence and apoptosis. *J Recept Signal Transduct.* 2015;35(6):600-4.
380 <https://doi.org/10.3109/10799893.2015.1030412>

- 381 12. Jochems R, Gaustad AH, Styrihave B, Zak LJ, Oskam IC, Grindflek E, et al. Follicular fluid steroid
382 hormones and in vitro embryo development in Duroc and Landrace pigs. *Theriogenology*. 2022;190:15-21.
383 <https://doi.org/10.1016/j.theriogenology.2022.07.004>
- 384 13. Billhaq DH, Lee S. The mechanisms of angiogenesis and apoptosis during the functional formation and
385 regression of the corpus luteum in the ovarian reproductive endocrine system. *Endocrines*. 2025;6(4):53.
386 <https://doi.org/10.3390/endocrines6040053>
- 387 14. Li D, Chen J, Guo J, Li L, Cai G, Chen S, et al. A phosphorylation of RIPK3 kinase initiates an intracellular
388 apoptotic pathway that promotes prostaglandin 2α -induced corpus luteum regression. *eLife*. 2021;10:1-29.
389 <https://doi.org/10.7554/eLife.67409>
- 390 15. Lee S-H, Lee S. Change of Ras and its guanosine triphosphatases (GTPases) during development and
391 regression in bovine corpus luteum. *Theriogenology*. 2020;144:16-26.
392 <https://doi.org/10.1016/j.theriogenology.2019.12.014>
- 393 16. Hennig A, Markwart R, Esparza-Franco MA, Ladds G, Rubio I. Ras activation revisited: role of GEF and
394 GAP systems. *Biol Chem*. 2015;396(8):831-48. <https://doi.org/10.1515/hsz-2014-0257>
- 395 17. Plendl J. Angiogenesis and vascular regression in the ovary. *Anat Histol Embryol*. 2000;29(5):257-66.
396 <https://doi.org/10.1046/j.1439-0264.2000.00265.x>
- 397 18. Min T-H, Lee S. The roles of Ral-interacting protein 76 and vascular endothelial growth factor in the ovarian
398 corpus luteum and tumor microenvironment. 2023. 10.20944/preprints202304.0538.v1
- 399 19. Schwentner L, Wöckel A, Herr D, Wulff C. Is there a role of the local tissue RAS in the regulation of
400 physiologic and pathophysiologic conditions in the reproductive tract? *J Renin-Angiotensin-Aldosterone*
401 *Syst*. 2011;12(4):385-93. <https://doi.org/10.1177/1470320311418140>
- 402 20. Snoeren EM. Female reproductive behavior. *Neuroendocrine regulation of behavior*: Springer; 2019:1-44.
403 <https://doi.org/10.1007/978-3-030-38720-4>
- 404 21. Guthrie H, Henricks D, Handlin D. Plasma estrogen, progesterone and luteinizing hormone prior to estrus
405 and during early pregnancy in pigs. *Endocrinology*. 1972;91(3):675-9. [https://doi.org/10.1210/endo-91-3-](https://doi.org/10.1210/endo-91-3-675)
406 675
- 407 22. Sykes M. Developing pig-to-human organ transplants. *Science*. 2022;378(6616):135-6.
408 <https://doi.org/10.1126/science.abo7935>

- 409 23. Mlyczyńska E, Kieżun M, Kurowska P, Dawid M, Pich K, Respekta N, et al. New aspects of corpus luteum
410 regulation in physiological and pathological conditions: involvement of adipokines and neuropeptides. *Cells*.
411 2022;11(6):1-47. <https://doi.org/10.3390/cells11060957>
- 412 24. Langin M, Mayr T, Reichart B, Michel S, Buchholz S, Guethoff S, et al. Consistent success in life-supporting
413 porcine cardiac xenotransplantation *NATURE*. 2018;568(7752):430–433. <https://doi.org/10.1038/s41586-018-0765-z>
- 415 25. Woad KJ, Robinson RS. Luteal angiogenesis and its control. *Theriogenology*. 2016;86(1):221-8.
416 <https://doi.org/10.1016/j.theriogenology.2016.04.035>
- 417 26. Przygodzka E, Kaczmarek M, Kaczynski P, Ziecik A. Steroid hormones, prostanoids, and angiogenic
418 systems during rescue of the corpus luteum in pigs. *Reproduction*. 2016;151(2):135-47.
419 <https://doi.org/10.1530/REP-15-0332>
- 420 27. Kurowska P, Mlyczyńska E, Dupont J, Rak A. Novel insights on the corpus luteum function: Role of vaspin
421 on porcine luteal cell angiogenesis, proliferation and apoptosis by activation of GRP78 receptor and MAP3/1
422 kinase pathways. *Int J Mol Sci*. 2020;21(18):1-17. <https://doi.org/10.3390/ijms21186823>
- 423 28. Waterman R. Lipid metabolism and in vitro production of progesterone and prostaglandin F during induced
424 regression of porcine corpora lutea. *Prostaglandins*. 1980;20(1):73-85. [https://doi.org/10.1016/0090-6980\(80\)90007-6](https://doi.org/10.1016/0090-6980(80)90007-6)
- 426 29. Seok E, Son M, Lee S, Cheong H-T, Lee S-H. The role of gonadotropins and growth factor in regulating Ras
427 during maturation in cumulus–oocyte complexes of pigs. *Animals*. 2025;15(14):2100.
428 <https://doi.org/10.3390/ani15142100>
- 429 30. Zhang Q, Wang Y, Bu Z, Zhang Y, Zhang Q, Li L, et al. Ras promotes germline stem cell division in
430 *Drosophila* ovaries. *Stem Cell Rep*. 2024;19(8):1205-16. <https://doi.org/10.1016/j.stemcr.2024.06.005>
- 431 31. Therachiyil L, Anand A, Azmi A, Bhat A, Korashy HM, Uddin S. Role of RAS signaling in ovarian cancer.
432 *F1000Res*. 2022;11:1-22. <https://doi.org/10.12688/f1000research.126337.1>
- 433 32. Gao S, Wang J, Wei L, Luo C, Qian F, Bo L, et al. Trehalose modulates OVRAS to improve oxidative stress
434 and apoptosis in KGN cells and ovaries of PCOS mice. *J Ovarian Res*. 2024;17(1):1-16.
435 <https://doi.org/10.1186/s13048-023-01337-5>
- 436 33. Sawada J, Urakami T, Li F, Urakami A, Zhu W, Fukuda M, et al. Small GTPase R-Ras regulates integrity
437 and functionality of tumor blood vessels. *Cancer Cell*. 2012;22(2):235-249.
438 <https://doi.org/10.1016/j.ccr.2012.06.013>

- 439 34. Livak KJ, Schmittgen TD. Analysis of relative gene expression data using real-time quantitative PCR and
440 the 2- $\Delta\Delta$ CT method. *methods*. 2001;25(4):402-408. <https://doi.org/10.1006/meth.2001.1262>
- 441 35. Snel B, Lehmann G, Bork P, Huynen MA. STRING: a web-server to retrieve and display the repeatedly
442 occurring neighbourhood of a gene. *Nucleic Acids Res*. 2000;28(18):3442-4.
443 <https://doi.org/10.1093/nar/28.18.3442>
- 444 36. Giacomini E, Pagliardini L, Minetto S, Pinna M, Kleeman F, Bonesi F, et al. The relationship between
445 CYP19A1 gene expression in luteinized granulosa cells and follicular estradiol output in women with
446 endometriosis. *The Journal of Steroid Biochemistry and Molecular Biology*. 2024;237:1-9.
447 <https://doi.org/10.1016/j.jsbmb.2023.106439>
- 448 37. Agca C, Ries JE, Kolath SJ, Kim J-H, Forrester LJ, Antoniou E, et al. Luteinization of porcine preovulatory
449 follicles leads to systematic changes in follicular gene expression. *Reproduction*. 2006;132(1):133-45.
450 <https://doi.org/10.1530/rep.1.01163>
- 451 38. Mlyczyńska E, Zaobidna E, Rytelawska E, Dobrzyń K, Kieżun M, Kopij G, et al. Expression and regulation
452 of visfatin/NAMPT in the porcine corpus luteum during the estrous cycle and early pregnancy. *Anim Reprod*
453 *Sci*. 2023;250:107212. <https://doi.org/10.1016/j.anireprosci.2023.107212>
- 454 39. Chen G, Bourneuf E, Marklund S, Zamaratskaia G, Madej A, Lundstrom K. Gene expression of 3 β -
455 hydroxysteroid dehydrogenase and 17 β -hydroxysteroid dehydrogenase in relation to androstenone,
456 testosterone, and estrone sulphate in gonadally intact male and castrated pigs. *J Anim Sci*. 2007;85(10):2457-
457 63. <https://doi.org/10.2527/jas.2007-0087>
- 458 40. Rasmussen MK, Ekstrand B, Zamaratskaia G. Regulation of 3 β -hydroxysteroid dehydrogenase/ Δ 5- Δ 4
459 isomerase: A Review. *Int J Mol Sci*. 2013;14(9):17926-42. <https://doi.org/10.3390/ijms140917926>
- 460 41. Tanaka J, Acosta TJ, Berisha B, Tetsuka M, Matsui M, Kobayashi S, et al. Relative changes in mRNA
461 expression of angiopoietins and receptors tie in bovine corpus luteum during estrous cycle and prostaglandin
462 F2 α -induced luteolysis: a possible mechanism for the initiation of luteal regression. *J Reprod Dev*.
463 2004;50(6):619-26. <https://doi.org/10.1262/jrd.50.619>
- 464 42. Glotzer M. The mechanism and control of cytokinesis. *Curr Opin Cell Biol*. 1997;9(6):815-23.
465 [https://doi.org/10.1016/S0955-0674\(97\)80082-8](https://doi.org/10.1016/S0955-0674(97)80082-8).
- 466 43. Bradshaw T, Simmons C, Ott RK, Armstrong AR. Ras/MAPK signaling mediates adipose tissue control of
467 ovarian germline survival and ovulation in *Drosophila melanogaster*. *Dev Biol*. 2024;510:17-28.
468 <https://doi.org/10.1016/j.ydbio.2024.02.009>

469 44. Nam Y, Cheong H-T, Lee S-H, Changes of gonadotropin receptors and Ras subfamily genes during maturation
470 in porcine cumulus cells. *J Anim Reprod Biotech.* 2025;40:50-57. <https://doi.org/10.12750/JARB.40.1.50>
471

ACCEPTED

472 **Tables**

473 Table 1. Primer condition for RT-PCR

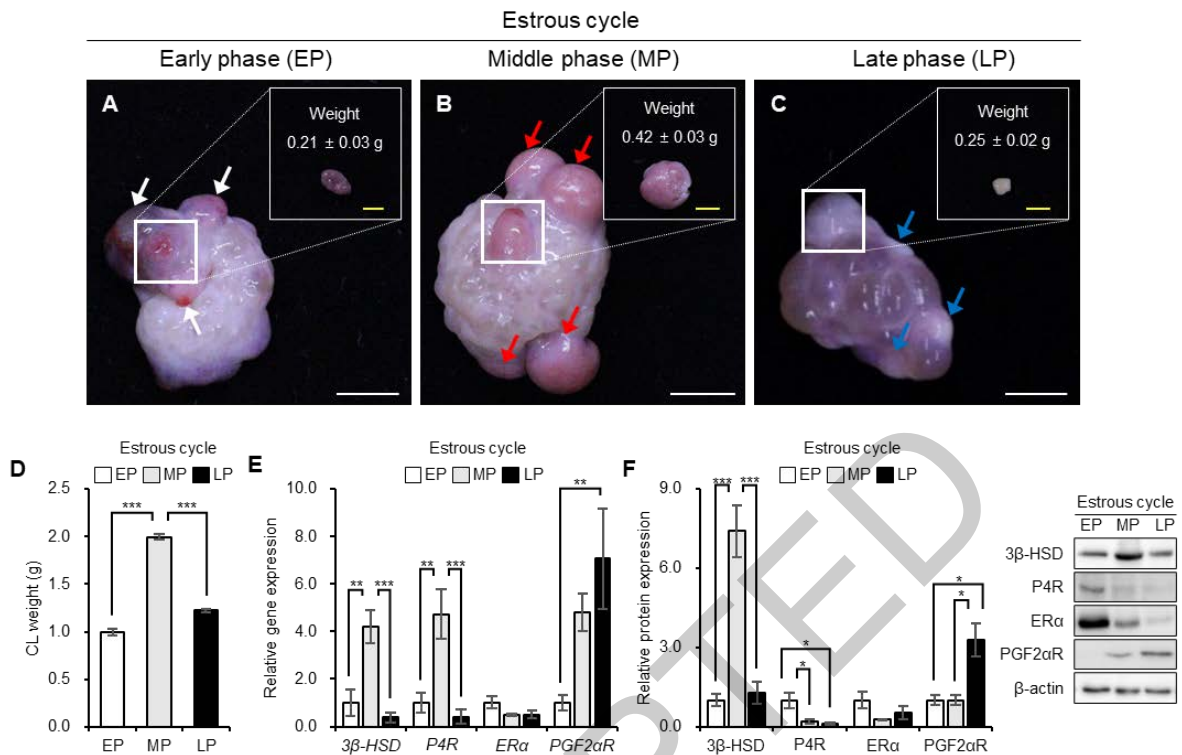
Genes	Sequence (5'-3')	Annealing temperature (°C)	Product size (bp)	Accession No.
<i>3β-HSD</i>	F: CCTTCCTGCTGGAAATAGTG R: TCTTGTAGGAGACGGTGAA	60	112	NM_001004049.2
<i>P4R</i>	F: GGACTAGGATGGAGATCCTATAA R: GCCACATGGTAAGGCATAA	60	124	NM_001166488.1
<i>ERα</i>	F: CTACCCTCTGTGACCTCTTC R: CCACACCAACACCAATAC	60	144	NM_001170521.1
<i>PGF2αR</i>	F: GCCATCACGGGAATTTCA R: GCAGGAGACGCACATTATAG	60	117	NM_214059.1
<i>VEGFA</i>	F: CAACTTCTGGGCTGTTCTC R: CCTCTCCTCTTCCTTCTCTT	60	147	NM_001435273.1
<i>VEGFR2</i>	F: TGTCTGCTCTGGGAAATA R: CAAGCATCGTCTGGTACATC	60	146	XM_013997943.2
<i>Ang1</i>	F: GAAGGAAACCGAGCCTATTC R: TCCCCTGTGACCCTTTA	60	91	NM_213959.1
<i>Tie2</i>	F: GACGTGTGCAGAACTCTATG R: CGCCAGCATTGTCTCATAA	60	102	XM_021062688.1
<i>H-Ras</i>	F: CCCTGACCATCCAGCTTAT R: GTCAATGACCACTTGCTTCC	60	89	XM_021082554.1
<i>K-Ras</i>	F: GATGGAGAAACCTGTCTCTTGG R: CTCATGTAAGTCCCTCATTG	60	80	XM_005653151
<i>N-Ras</i>	F: TCCCACCATAGAGGACTCTTAC R: TTCGCCTGTCCTCATGTATTG	60	130	NM_001044537.1
<i>R-Ras</i>	F: CCTGCTGGTGTGTTGCCATTA R: GAAGTCATCTCGGTCCTTGACT	60	94	XM_003355998.3
<i>RASA1</i>	F: TCCAGAACAAGCAGAGGATTG R: GACCTGACGCAGACGTTTAT	60	97	XM_021084515.1
<i>SOS1</i>	F: TCCTCCTGCTTCTGGTGCTTCTAG R: AAAGACGGTATCGCTGCTTGAGTG	60	210	XM_021087589.1
<i>NF1</i>	F: GCAGTTCAGACCCTAGTTTAC R: TGTTGGCTGGGATACATAACC	60	123	XM_021067460.1
<i>ERK1</i>	F: CCACATCTGCTACTTCCTCTAC R: GGCCACATATTCGTCGAAGA	60	196	HM745137
<i>MAPK1</i>	F: CCCTCACAAGAGGATTGAAGTAG R: GATCTGTATCCTGGCTGGAATC	60	189	NM_001198922
<i>CDK1</i>	F: GGTGTTCCCTAGTACTGCCATTC R: GAATCCATGAACTGACCAGGAG	60	179	NM_001159304.2
<i>CCNB1</i>	F: GTGTCAGGCTTTCTCTGATGT R: CCAGTCAATTAGGATGGCTCTC	60	199	NM_001170768.1
<i>TNFR1</i>	F: GAACGCAGACTGCAAGAA R: CTAAGCCAACGAAGAGGAAG	60	137	NM_213969.1
<i>Bax</i>	F: CTCAGGATGCATCTACCAAGAA R: GCACCAGTTTACTGGCAAAG	60	213	XM_003127290.5
<i>Bcl2</i>	F: AGGGCATTGAGTACCTGAC R: CGATCCGACTACCAATACC	60	193	XM_021077293.1
<i>Casp3</i>	F: ACCGAAAGGTAGCAGTAGA R: GTGAGCATGGACACAATACA	60	91	NM_214131.1
<i>β-actin</i>	F: TCTGGCACCACACCTTCTA R: TCTTCTCACGGTTGGCTTTG	60	102	XM_021086047.1

474

Table 2. List of antibodies for western blot

1st Antibody (Ab)	Cat. No.	Host species	Company	1 st Ab dilution	Secondary antibody	2 nd Ab dilution
3 β -HSD	sc-515120	Mouse	SCBT	1:1000	goat anti-mouse IgG-HRP	1:10000
P4R	sc-539	Rabbit	SCBT	1:1000	goat anti-rabbit IgG-HRP	1:10000
ER α	sc-8005	Mouse	SCBT	1:1000	goat anti-mouse IgG-HRP	1:10000
PGF2 α R	sc-33364	Goat	SCBT	1:1000	donkey anti-goat IgG-HRP	1:10000
VEGF-D	sc-25784	Rabbit	SCBT	1:1000	goat anti-rabbit IgG-HRP	1:10000
Ang-4	sc-377497	Mouse	SCBT	1:1000	goat anti-mouse IgG-HRP	1:10000
Tie-2	sc-293414	Mouse	SCBT	1:1000	goat anti-mouse IgG-HRP	1:10000
ERK1/2	4696S	Mouse	Cell Signaling	1:2000	goat anti-mouse IgG-HRP	1:10000
p-ERK1/2	4370S	Rabbit	Cell Signaling	1:2000	goat anti-rabbit IgG-HRP	1:10000
CCNB1	554178	Mouse	BD	1:1000	goat anti-mouse IgG-HRP	1:10000
TNFR1	sc-8436	Mouse	SCBT	1:1000	goat anti-mouse IgG-HRP	1:10000
Bax	sc-23959	Mouse	SCBT	1:1000	goat anti-mouse IgG-HRP	1:10000
Bcl2	sc-7382	Mouse	SCBT	1:1000	goat anti-mouse IgG-HRP	1:10000
Casp3	sc-56046	Mouse	SCBT	1:1000	goat anti-mouse IgG-HRP	1:10000
H-Ras	sc-35	Rat	SCBT	1:1000	goat anti-rat IgG-HRP	1:10000
K-Ras	#71835	Rabbit	Cell Signaling	1:1000	goat anti-rabbit IgG-HRP	1:10000
R-Ras	#8446	Rabbit	Cell Signaling	1:1000	goat anti-rabbit IgG-HRP	1:10000
NF1	#14623	Rabbit	Cell Signaling	1:1000	goat anti-rabbit IgG-HRP	1:10000
RASA1	EP536Y	Rabbit	Abcam	1:1000	goat anti-rabbit IgG-HRP	1:10000
SOS1	#5890	Rabbit	Cell Signaling	1:1000	goat anti-rabbit IgG-HRP	1:10000
β -Actin	sc-47778	Mouse	SCBT	1:1000	goat anti-mouse IgG-HRP	1:10000

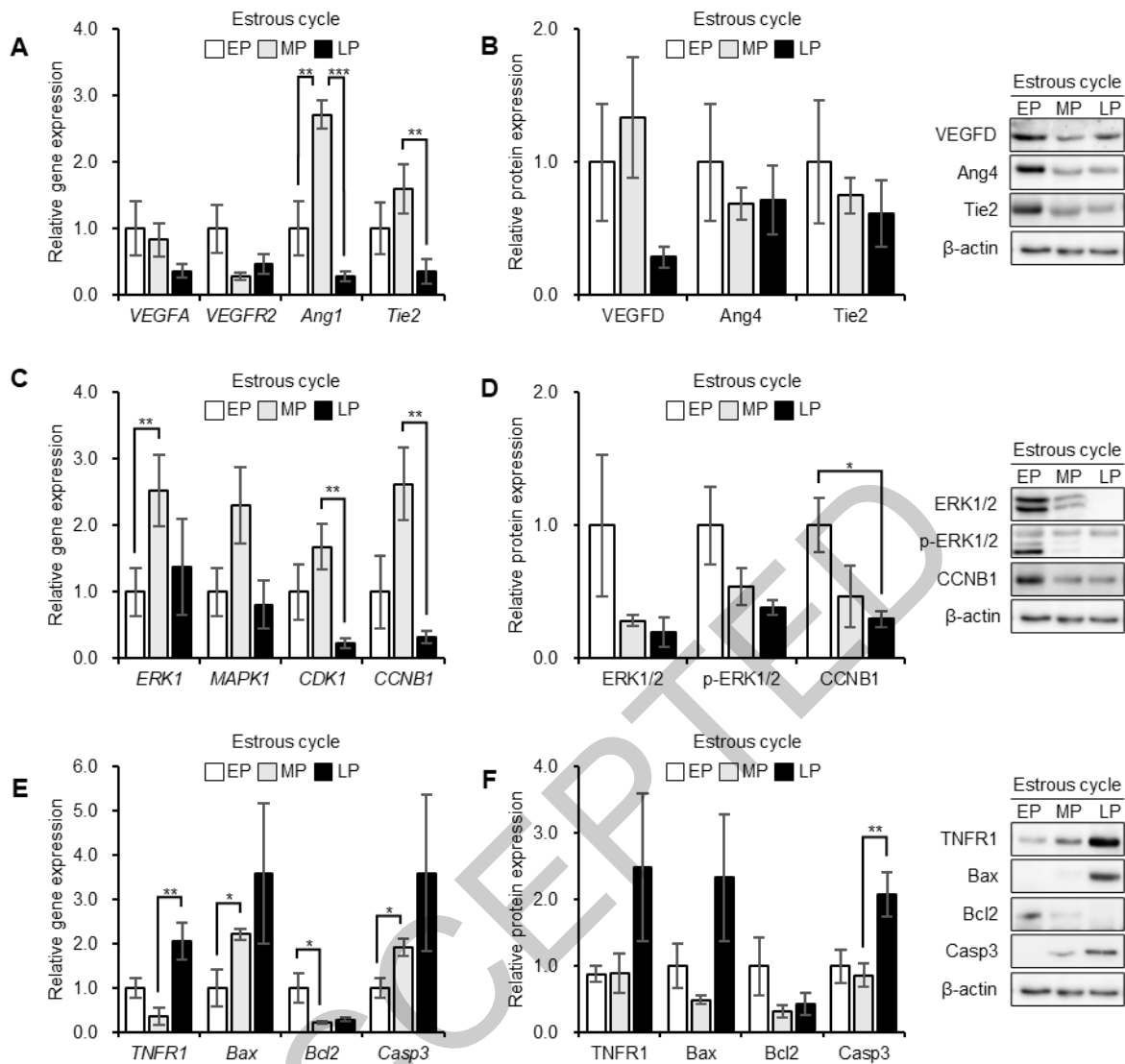
477 **Figures**



478

479

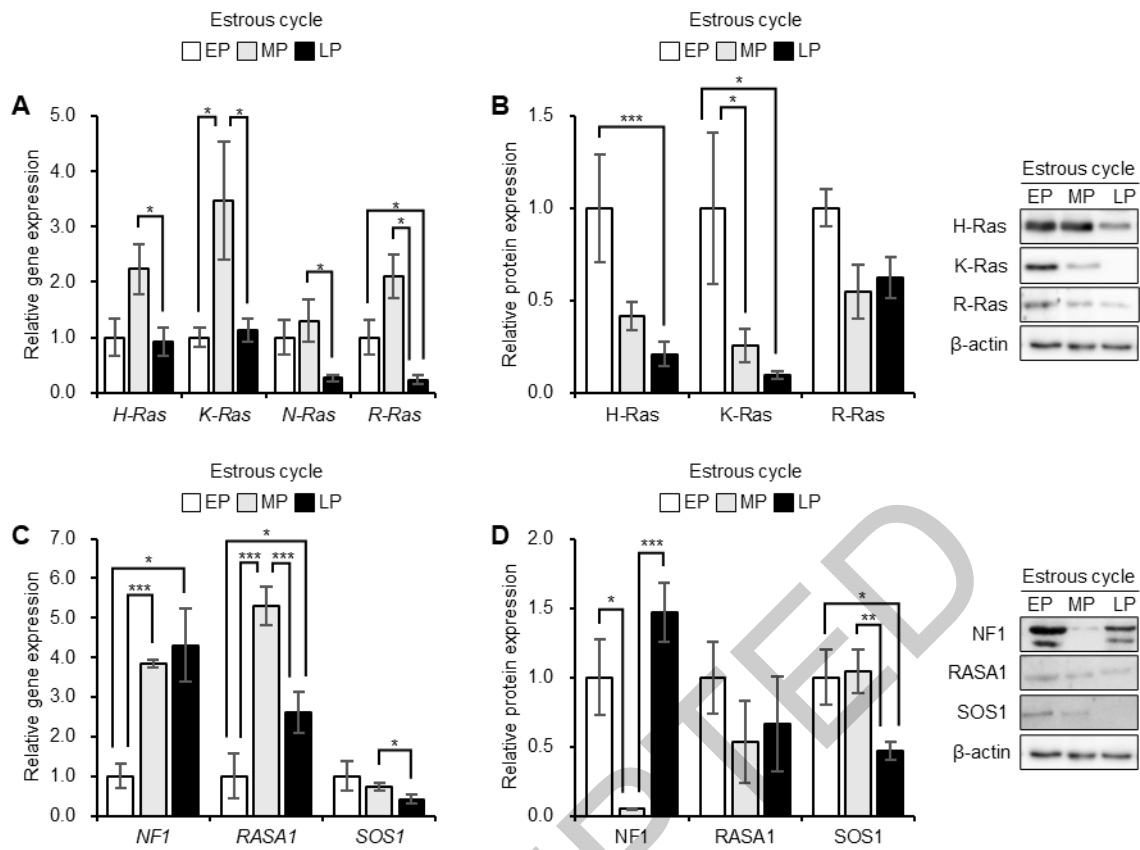
480 Fig. 1. Morphological characteristics, tissue weight, and expression of the steroid hormone receptors in the porcine
 481 ovary during the estrous cycle. Representative images revealing the shape of the prominent corpus luteum (CL)
 482 in porcine ovaries at the early (EP; A; white arrows), middle (MP; B; red arrows), and late phases (LP; C; blue
 483 arrows) of the estrous cycle. The white scale bar indicates 1.0 cm, and the yellow scale bar indicates 0.5 cm. White
 484 boxes represent enlarged areas of the CL. The tissue weight of the CL during the estrous cycle (D); alterations in
 485 *3β-hydroxysteroid dehydrogenase (3β-HSD)*, *progesterone receptor (P4R)*, *estrogen receptor alpha (ERα)*, and
 486 *prostaglandin F2 alpha receptor (PGF2αR)* mRNA (E) and protein (F), mRNA and protein expression of the MP
 487 and LP was normalized to that of the EP. Data are presented as the mean ± standard error of the mean. Significant
 488 differences between groups are indicated as * $p < 0.05$, ** $p < 0.01$, and *** $p < 0.001$.



489

490 Fig. 2. Changes in the vascular endothelial growth factor A (VEGFA), vascular endothelial growth factor receptor
 491 2 (VEGFR2), angiopoietin 1 (Ang1), and Tie2 mRNA (A); vascular endothelial growth factor-D (VEGFD),
 492 angiopoietin 4 (Ang4), and Tie2 protein (B); extracellular signal-regulated kinase 1 (ERK1), mitogen-activated
 493 protein kinase 1 (MAPK1), cyclin-dependent kinase 1 (CDK1), and cyclin B1 (CCNB1) mRNA (C); ERK1/2,
 494 phosphorylated ERK1/2 (p-ERK1/2), and CCNB1 protein (D); tumor necrosis factor receptor 1 (TNFR1), Bax,
 495 Bcl2, and caspase 3 (Casp3) mRNA (E) and protein (F) at the early (EP), middle (MP), and late phases (LP).
 496 mRNA and protein expression of the MP and LP was normalized to that of the EP. Data are presented as the mean
 497 \pm standard error of the mean. Significant differences between the groups are indicated as * $p < 0.05$, ** $p < 0.01$, and
 498 *** $p < 0.001$.

499



500

501

502 Fig. 3. Changes in the *H-Ras*, *K-Ras*, *N-Ras*, and *R-Ras* mRNA (A); H-Ras, K-Ras, and R-Ras protein (B);

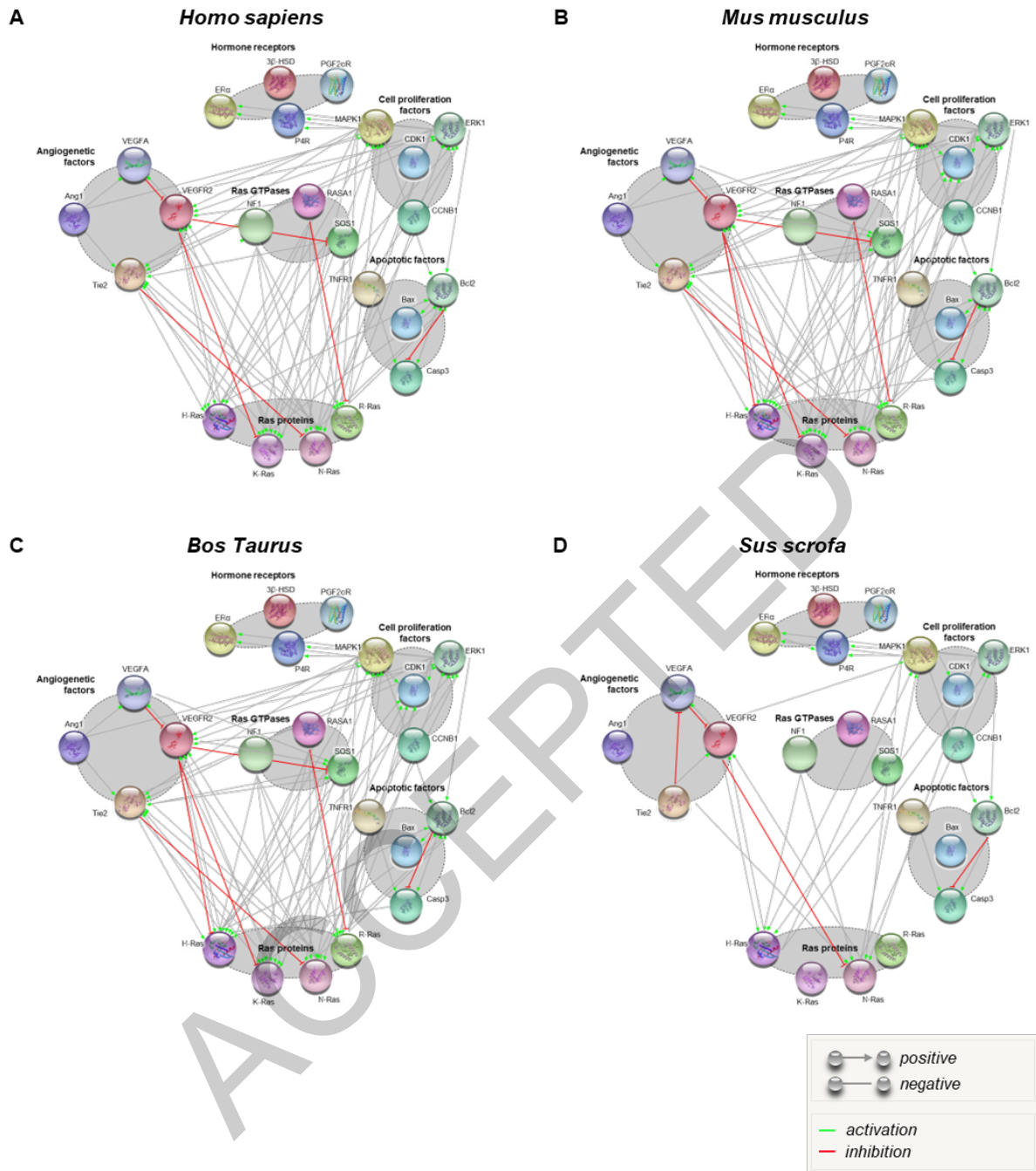
503 neurofibromin 1 (NF1), Ras GTPase-activating protein 1 (RASA1), and son of sevenless homolog 1 (SOS1)

504 mRNA (C) and protein (D) at the early (EP), middle (MP), and late phases (LP). mRNA and protein expression

505 of the MP and LP was normalized to that of the EP. Data are presented as the mean \pm standard error of the mean.

506 Significant differences between the groups are indicated as * $p < 0.05$, ** $p < 0.01$, and *** $p < 0.001$.

507



508
509
510
511
512
513
514

Fig. 4. Construction and analysis of the protein-protein interaction (PPI) network using the Search Tool for the Retrieval of Interacting Genes (STRING) database. Each edge color indicates a different method of PPI prediction. Network plot of top15 interaction protein in *Homo sapiens* (A), *Mus musculus* (B), *Bos Taurus* (C), and *Sus scrofa* (D). Proteins are represented as the respective national Center for Biotechnology Information (NCBI) gene names.